groundwater. The findings are significant as the area falls in the potential mining and industrial belt of Chhattisgarh, emphasizing a large population may be at potential risk. The rock and water interaction with accompanying ion exchange processes in micas and clay minerals appear to be the primary mechanism for high concentration of F^- in groundwater. Systematic study needs to be undertaken in the Gondwana rocks in the surrounding area, with an emphasis on the coal-bearing Barakar Formation, to delineate unsafe zones.

1. Cao, J., Zhao, Y., Lin, J. W., Xirao, R. D. and Danzeng, S. B., Environmental fluoride in Tibet. *Environ. Res.*, 2000, **83**, 333–337.
2. Handa, B. K., Geochemistry and genesis of fluoride containing groundwater in India. *Ground Water*, 1975, **13**, 275–281.
3. Ripa, L. W., A half-century of community water fluoridation in the United States: review and commentary. *J. Public Health Dent.*, 1993, **53**, 17–44.
4. USPHS, Drinking water standards. United States Public Health Services, Washington DC, 1987.
5. WHO, Guidelines for drinking water quality, World Health Organization, Geneva, 1984.
6. Chaturvedi, A. K., Yadva, K. P., Yadava, K. C, Pathak, K. C. and Singh, V. N., Deflouridation of water by adsorption on fly ash. *Water, Air, Soil Pollut.*, 1990, **49**, 51–61.
7. Rajgopal, R. and Tobin, G., Fluoride in drinking water: a survey of expert opinions. *Environ. Geochem. Health*, 1991, **13**, 3–13.
8. Meenakshi and Maheshwari, R. C., Fluoride in drinking water and its removal. *J. Hazard. Mater*., 2006, **137**, 456–463.
9. BIS, Indian Standards for drinking water – specification (IS 10500:1991), Bureau of Indian Standards, New Delhi, 1991.
10. Subba Rao, N. and Devdas, D. J., Fluoride incidence in groundwater in an area of peninsula India. *Environ. Geol.*, 2003, **45**, 243–251.
11. Saxena, V. K. and Ahmad, S., Inferring the chemical parameter for the dissolution of fluoride in groundwater. *Environ. Geol*., 2002, **25**, 475–481.
12. Chae, G. Y., Seong, T. M., Bernhard, K., Kyoung-Ho, K. and Seong-Yong, K., Fluorine geochemistry in bedrock groundwater of South Korea. *Sci. Total Environ*., 2007, **385**, 272–283.
13. UNICEF, State of the art report on the extent of fluoride in drinking water and the resulting endemicity in India. Fluorosis Research and Rural Development Foundation for UNICEF, New Delhi, 1999.
14. WHO, Fluoride in drinking water, World Health Organization, Geneva, 2006.
15. Pillai, K. S. and Stanley, V. A., Implication of fluoride – an endless uncertainty. *J. Environ. Biol.*, 2002, **23**, 81–87.
16. Mall, R. K., Gupta, A., Singh, R., Singh, R. S. and Rathore, L. S., Water resources and climate change: an Indian perspective. *Curr. Sci*., 2006, **90**, 1610–1626.
17. Ahmed, S., Bertrand, F., Saxena, V., Subramaniyam, K. and Touchard, F., A geostatistical method of determining priority of measurement wells in a fluoride monitoring network in an aquifer. *J. Appl. Geochem*., 2002, **4**, 576–585.
18. Vikas, C., Kushwaha, R. K. and Pandit, M. K., Hydrochemical status of groundwater in District Ajmer (NW India) with reference to fluoride distribution. *J. Geol. Soc. India*, 2009, **73**, 773–784.
19. Beg, M. K., Geospatial analysis of fluoride contamination in groundwater of Tamnar area, Raigarh district, Chhattisgarh state. M Sc thesis, ITC, The Netherlands, 2009.
20. APHA, Standard methods for the examination of water and wastewater. American Public Health Association, Washington DC, 1992.
21. Raju, N. J., Dey, S. and Das, K., Fluoride contamination in groundwaters of Sonbhadra District, Uttar Pradesh, India. *Curr. Sci.*, 2009, **96**, 699–702.
22. Apambire, W. B., Boyle, D. R. and Michel, F. A., Geochemistry, genesis and health implication of fluoriferous groundwater in the upper regions, Ghana. *Environ. Geol.*, 1997, **33**, 13–24.

ACKNOWLEDGEMENTS. This study forms a part of the M Sc research carried out by M.K.B. under the joint M Sc (Geohazards) course programme of the Indian Institute of Remote Sensing (IIRS), Dehra Dun and International Institute for Geo-information Science and Earth Observation, The Netherlands. We thank the Director, National Remote Sensing Centre, Hyderabad, and the Dean, IIRS for providing the necessary facilities and support. M.K.B. is grateful to Dr P. K. Bhat, Director General, Chhattisgarh Council of Science and Technology, Raipur for support and encouragement. We thank Dr K. S. Patel, Dhananjay Sahu, Dr Gopal Krishan, Mahendra Singh and Dr P. K. Mukherjee for help in chemical, petrographic and XRD analyses and the officials of the Public Health Engineering Department of Chhattisgarh, for assistance during ground campaigns. We also thank the two reviewers for their comments which helped improve the manuscript.

Received 1 September 2009; revised accepted 7 December 2010

Seismic site characterization using *Vs*30 and site amplification in Gandhinagar region, Gujarat, India

B. Sairam*, B. K. Rastogi, Sandeep Aggarwal, Mukesh Chauhan and Uday Bhonde

Institute of Seismological Research, Raisan, Gandhinagar 382 009, India

Gujarat is prone to earthquake hazard of different levels from moderate to high, assigned as zones II–V in the seismic zoning map of India. Many multistorey buildings collapsed in Ahmedabad city at a distance of 225 km from the location of the 2001 Bhuj earthquake. Gandhinagar falls in zone III where an intensity of VII or VIII from the regional large earthquakes or local earthquakes of magnitude 6 can be expected; which can damage single and multistorey buildings. Thus, there is a need for site characterization and seismic hazard mapping of the area. Shear-wave velocities were measured using the MASW technique at 63 sites in and around Gandhinagar. Based on *Vs*30 in most of Gandhinagar the soils have been classified as D-type (180–360 m/s) in accordance with the NEHRP provision, except the northern part of the city (sites 27, 51, 53 and 54), where *Vs*30 values larger than 360 m/s qualify the area as a NEHRP class C-type soil (360–760 m/s). However, nearly the whole of Gandhi-

*For correspondence. (e-mail: sairambharat@rediffmail.com)

nagar soil has *Vs* > 250 m/s, that is considered to be strong. Further for the estimation of site amplification of the study area, we have used earthquake as well as microtremor records. Site amplification up to 4.4 was observed in the frequency range 0.4–2 Hz. The frequency range 3–10 Hz shows amplification up to 2.4 times at some sites. The frequency range 0.4–2.0 Hz falls in the natural frequency range of multistorey buildings with more than three floors. It is inferred from shear-wave velocity measurements and site amplification that multistorey buildings of more than three floors in this region require careful designing.

Keywords: Earthquake, seismic hazard mapping, shear-wave velocity, site amplification.

GUJARAT has experienced great earthquakes in the past, the last being on 26 January 2001 that struck Bhuj. The Bhuj earthquake (M_w 7.7) was one of the most destructive intraplate earthquakes of India, killing about 20,000 people and injuring many more[1]. An intensity of XI close to the epicentre has been estimated[2] on a Modified Mercalli Intensity (MMI) scale. The earthquake caused severe damage not only in the epicentral region, but spread over 350 km, including major cities like Ahmedabad, Bhuj, Rajkot, Anjar, Gandhidham, Morbi and Surendranagar. The whole of Gujarat region is prone to earthquake hazard of different levels from moderate to high, assigned as zones II–V in the seismic zoning map of India. Gandhinagar area lies in zone III where an earthquake of magnitude 6 can be expected, which can damage single or multistorey buildings. Also, there is danger to multistorey buildings from the future great earthquakes in Kachchh seismic zone. Medium to high seismic risk exists at Gandhinagar from the local and regional strong earthquakes.

Several earthquakes like Mexico (1985), San Francisco (1989) and Los Angeles (1995) have established the fact that local site conditions play a significant role in the amplification of ground motion, especially in the areas that are located on unconsolidated young sedimentary materials[3]. The intensity of ground motion is a function of earthquake magnitude and distance from the seismic source, as well as local soil condition, topography and geological condition, etc. In general, softness of the surface layer not only tends to amplify ground motion at certain frequencies, but also extends the duration, which may cause further damage during earthquakes. The fundamental phenomenon responsible for the amplification of motion over soft sediments is the trapping of seismic waves due to the impedance contrast between sedimentary deposits and the underlying bedrock.

The damage due to an earthquake is generally large over soft sediments than on firm bedrock outcrops. It is also a well-known fact that in most cases site amplification/shaking is stronger in low shear-wave velocity areas. Mapping the seismic hazard at local scales to incorporate the effects of local ground conditions is the essence of microzonation. Shallow shear-wave velocity structure to a depth of 30 m is a key parameter to evaluate the near-surface stiffness and for characterizing the given site. The classification of sites based on *Vs*30 is given by the National Earthquake Hazard Reduction Program (NEHRP)[4] and Uniform Building Code[5], USA. These codes were developed after strong earthquakes occurred in USA, Japan, Europe and other countries. In general, the parameters describing the site effects in seismic codes are expressed through soil characterization and spectral amplification factor.

Multichannel Analysis of Surface Waves (MASW)[6,7] is a non-invasive method developed to estimate shear-wave velocity profile from surface wave energy. Measurements of phase velocity of Rayleigh waves of different frequencies can be used to determine a velocity depth profile.

Gandhinagar falls in zone III in the seismic zoning map of India where intensity VII or VIII from the regional large earthquake or local earthquake of magnitude 6 can be expected; this can damage single to multistorey buildings. There is a need for site characterization and seismic hazard mapping of the area. For this, we have carried out the MASW test at 63 sites for 2D shear-wave velocity measurements in and around Gandhinagar. Further, site amplification for this study region has been computed using the earthquake records (at 9 sites) and microtremor records (at 30 sites). We have used broadband seismographs (BBS) for recording earthquakes and microtremors at a sampling rate of 100 samples/s. Microtremors were recorded for 4 hours at each site.

Gandhinagar is situated on the western bank of Sabarmati, which is a non-perennial river. The city is oriented parallel to the Sabarmati River cutting through the alluvial plains of the Cambay graben. Surface deposits are recent sediments filled up in the graben structure. The average thickness of the Quaternary sediments up to the Tertiary clay varies between 400 and 500 m. Geomorphologically, the city is situated on the meanders of the Sabarmati River. Floodplains cover the entire Gandhinagar region, where the silty sediments and sand are exposed on the surface.

The MASW technique is employed to utilize the dispersive properties of Rayleigh waves for imaging the subsurface layers. The entire process of MASW consists of three major steps: (i) acquisition of ground roll data (Rayleigh surface waves); (ii) construction of a dispersion curve, a plot of phase velocity versus frequency, and (iii) inversion of the shear-wave velocity (*Vs*) profile from the calculated dispersion curve. Integrating the MASW technique with common mid point (CMP) style data acquisition permits the generation of laterally continuous 2D cross-section of the shear-wave velocity profile[6]. In seismic surveys, when a compressional wave source is used, more than two-thirds of the total seismic energy is imparted into Rayleigh waves[8], the principal component of ground roll.

The advances in surface wave analysis that have come with the development of the MASW method permit confident estimates of shear-wave velocities (*Vs*). The practical application of MASW has provided reliable correlations to drill data[9]. The MASW method can be applied to seismic characterization of pavements[10,11], to study Poisson ratio[12], seismic study of sea-bottom sediments[12,13], mapping bedrock surface[14], and detecting dissolution features[15]. Sinkholes and related subsidence features, obscured by suburban development and not detectable using other geophysical methods because of power-line and mechanical noise, reinforced concrete, and non-invasive testing requirements, were identified in a residential area in western Florida[15].

MASW being a relatively recent technology in geotechnological engineering and engineering geophysics, is gaining greater importance in the recent past. It attracted the attention of earth scientists because this method is a powerful, rapid and cost-effective tool for estimating accurate shear-wave velocity of structures. This method is also useful to a scientist, a geotechnical engineer or a seismologist who needs a quick assessment of site characterization or a reliable velocity structure, which is used in earthquake ground motions.

MASW is a geophysical method which generates a shear-wave velocity (*Vs*) profile (i.e. *Vs* versus depth) by analysing Rayleigh-type surface waves on a multichannel record. The term 'multichannel record' indicates a seismic dataset acquired using a recording instrument with multiple channels. A 48 channel Geode Seismograph and Seismodule Controller Software (SCS), Geometrics Inc., USA, has been used to acquire data in this study. Data were acquired using standard CMP roll-along technique to achieve a continuous shot gather. Vertically stacked 15 impacts of a 10 kg hammer on a metal plate were used as a source to generate seismic waves. These waves were recorded by 24 vertical geophones/receivers of 4.5 Hz planted at a 2 m interval along the profile line.

The MASW test was carried out at 63 locations in the study area. Locations of the testing sites are shown in Figure 1. An effective result of MASW depends on signal-to-noise ratio (S/N) of surface waves. The optimum field parameters such as the source to the first and last receiver, receiver spacing and the spread length of survey lines were selected in such a way that the highest S/N ratio and required depth (more than 30 m) of information could be obtained. Typical shotgather record using source to first receiver distance of 4 m with record length of 0.5 s is shown in Figure 2.

The generation of a dispersion curve is an important step in the MASW method. A dispersion curve is generally displayed as a function of phase velocity versus frequency. Each shotgather generated one dispersion curve. Care was taken to ensure that the spectral properties of the $t - x$ (t is the time and x the offset) data (shotgathers) were consistent with the maximum and minimum $f - Vc$ values (f is the frequency and Vc the phase velocity of surface waves) contained in the dispersion curve. The lowest analysed frequency in this dispersion curve is around 5 Hz and the highest frequency of 35 Hz has been considered. A typical dispersion curve is shown in Figure 3. Each dispersion curve obtained for the corresponding

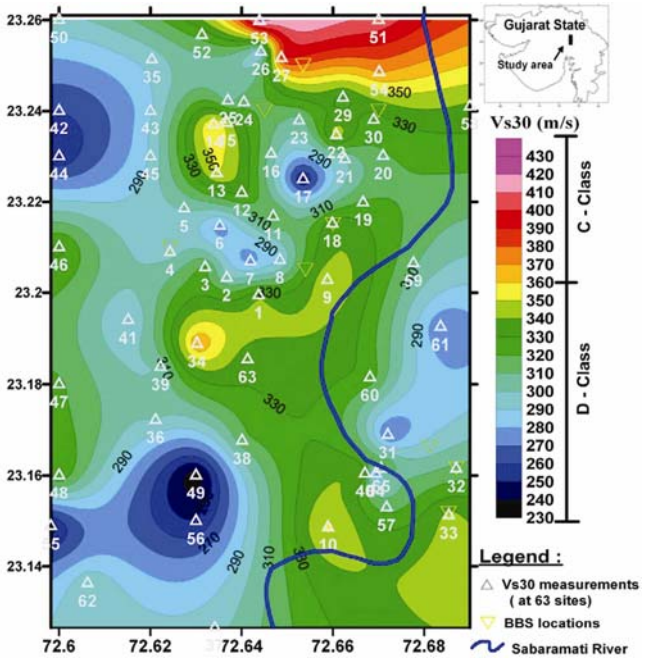

Figure 1. Contour map of *Vs*30 and site characterization in the study area, Gandhinagar, Gujarat, India.

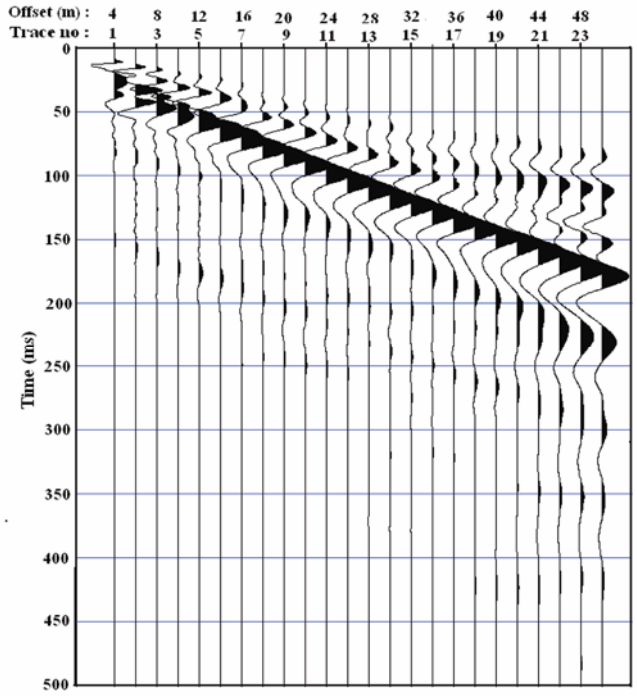

Figure 2. Typical 24-channel shotgather recorded in the study area.

locations has a very high S/N ratio of 0.85 and above. Each dispersion curve was individually inverted into an $x - Vs(z)$ trace ($Vs(z)$ is shear-wave velocity variation with depth at location x). Gathering all $x - Vs(z)$ traces into a shot station in sequential order results in a 2D grid of the shear-wave velocity profile. A typical 2D velocity profile is shown in Figure 4. Multi-channel records were analysed with *SurfSeis* (a propriety software package of the Kansans Geological Survey, USA), which facilitates the use of MASW with a continuous profiling technique.

The shear-wave velocity was averaged over the top 30 m layers (surface to a depth 30 m) and computed using the formula

$$Vs30 = \frac{30}{\sum_{i=1,N} \frac{di}{Vsi}}, \quad (1)$$

where di is the thickness of the ith layer (in m), Vsi the shear-wave velocity in the ith layer (in m/s) and shear-wave velocities of N layers exist in the top 30 m. Modern seismic codes like NEHRP[4], Federal Emergency Management Agency[16], Uniform Building Code[5] and International Building Code[17] use $Vs30$ for site characterization. $Vs30$ for all the sites was calculated using eq. (1), and was found to range from 230 to 450 m/s for the study region.

Site amplification for the study region has been computed using the earthquake records (at 9 sites) and microtremors (at 30 sites) records. We have used BBS for recording the earthquakes and microtremors at a sampling rate of 100 samples/s. Microtremors were recorded for 4 hours at each site. The sites are well distributed in and around Gandhinagar, so that site amplification computed from them will represent the whole study area. In H/V method, the assumption is that only the horizontal and not the vertical component is amplified. Hence the H/V ratio gives site amplification.

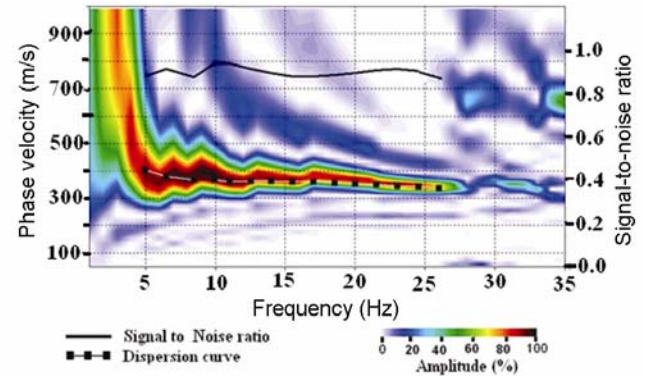

Figure 3. Typical dispersion curve.

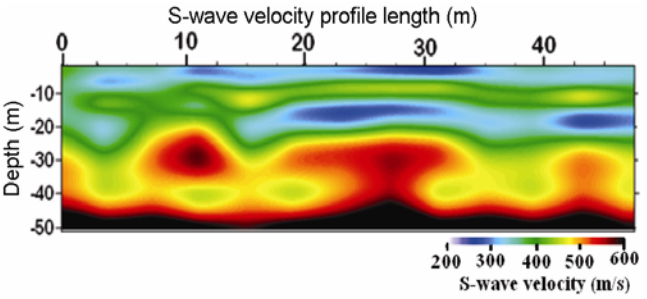

Figure 4. Typical 2D velocity profile.

In the present study, H/V was calculated using earthquake records and microtremor data. FFT was applied to the signal of the three components to obtain three spectral amplitudes. The spectra were then smoothed following Konno and Ohmachi[18], with a bandwidth parameter of 40 and arithmetical average was applied to the three spectral amplitudes. The mathematical formulation of the H/V ratio method is based on a spectral ratio (R_{hv}) between the smoothed horizontal components and the smoothed vertical component:

$$R_{hv} = \frac{\{(s_{NS}(f)^2 + s_{EW}(f)^2)/2\}^{1/2}}{s_v(f)}. \quad (2)$$

where $s_{NS}(f)^2$ is North-South component, $s_{EW}(f)^2$ East-West component and $s_v(f)$ vertical component of BBS.

In order to obtain a site response, a resultant horizontal component was calculated for the two horizontal components ($s_{NS}(f)$ and $s_{EW}(f)$) and divided by the vertical component ($s_v(f)$) using eq. (2). Thus, for each of the n windows the distribution of $\log_{10}(H/V)$ was obtained as a function of frequency. The average H/V (H/V_{avg}) overall selected windows (n) was obtained using the formula

$$H/V_{avg} = \frac{\log_{10}(H/V)}{n_{windows}}. \quad (3)$$

For the microtremor, a time window of 70 s was used. For earthquake records 10.5 s time window starting from 0.5 s before S-wave phase arrival was used for all components. This time-window length was chosen to best contain most of the high-amplitude of S-wave energy of earthquake records. As pointed out by Bonilla *et al.*[19], using longer time results in better spectral resolution at the cost of including the scattered and reflected energy as well as surface waves in the spectra. Bonilla *et al.*[19] and Field and Jacob[20] found no statistical variation in site response computed with spectra of different time windows. However, Castro *et al.*[21] suggested that S-waves could be contaminated by surface waves at larger epicentral distance, which demands variable time windows for the estimation of the H/V spectral ratio using S-waves. Bonilla *et al.*[22] drew attention to the fact that a significant site response can be associated with the vertical component resulting from S to P-wave conversion at the weathered

Table 1. Site amplification using earthquake records

Site location	Amplification in frequency range			Peak amplification	*Vs*30 (m/s)
	0.1–1 Hz	1–3 Hz	3–10 Hz		
Site-4	1.0–3.0	1.4–3.4	0.5–1.0	3.4	295
Site-8	0.8–1.9	1.0–3.8	0.7–1.5	3.8	288
Site-17	0.2–4.0	0.9–4.4	0.7–1.3	4.4	246
Site-18	1.2–3.3	1.0–3.3	0.4–1.1	3.3	330
Site-24	1.2–2.6	1.3–3.4	0.5–1.9	3.4	317
Site-30	1.3–1.8	0.8–3.6	0.8–2.0	3.6	320
Site-31	1.6–4.4	1.6–2.6	0.4–1.1	4.4	260
Site-32	2.0–3.0	1.1–3.1	1.0–1.5	3.1	320
Site-33	0.9–1.9	1.1–2.7	0.4–1.1	2.7	343

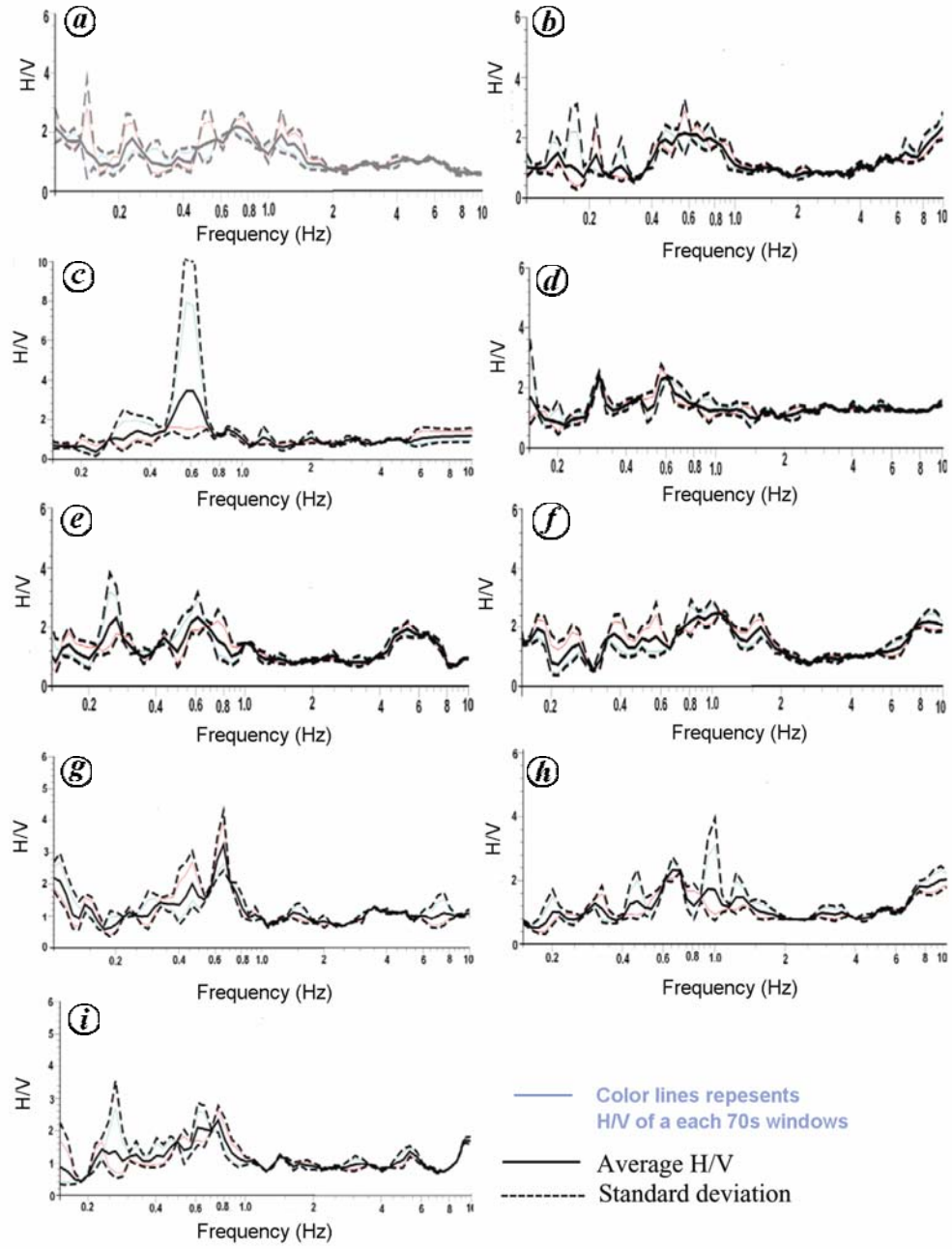

Figure 5. Site amplification (*H*/*V*) computed by Nakamura method using microtremors at nine sites. ***a***, Site-4; ***b***, Site-8; ***c***, Site-17; ***d***, Site-18; ***e***, Site-24; ***f***, Site-30; ***g***, Site-31; ***h***, Site-32 and ***i***, Site-33.

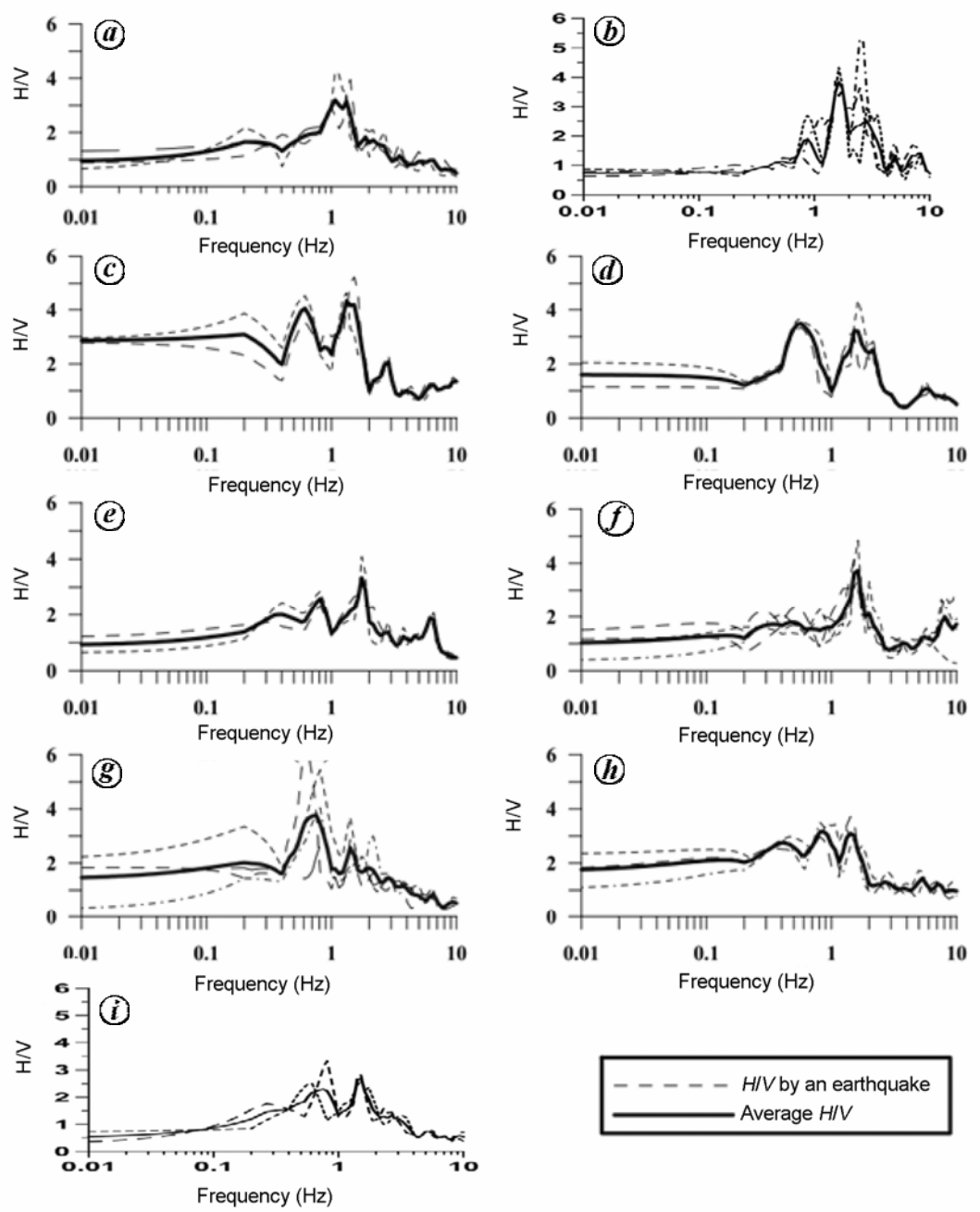

Figure 6. Site amplification (*H*/*V*) by Nakamura method using earthquake records at nine sites. ***a***, Site-4; ***b***, Site-8; ***c***, Site-17; ***d***, Site-18; ***e***, Site-24; ***f***, Site-30; ***d***, Site-31; ***g***, Site-32 and ***h***, Site-33.

granite boundary, and that this violates the basic assumption behind the *H*/*V* method. Nevertheless, the *H*/*V* method has been widely used to estimate a site response of many areas.

It has been observed that shear-wave velocities measured using MASW correlate well with geological settings. It is evident from the site study that the soil is stiff from the surface to 12 m depth (*Vs* ~ 180–360 m/s), followed by dense soil to a depth of 30 m (velocity ranging from 360 to 500 m/s). In most of the study areas of Gandhinagar *Vs*30 falls in the range 250–350 m/s, except the northern portion (north of sites 26–30) which has velocity of 360–430 m/s. Based on *Vs*30 of the soils, a major portion of the study area is predominantly classified as D-type (180–360 m/s; Figure 1) in accordance with the 1997 NEHRP provision. Sites located in the northern part of the city (sites: 27, 51, 53 and 54) have *Vs*30 values larger than 360 m/s, thereby qualifying the soils as NEHRP class C-type (360–760 m/s; Figure 1).

Site response ranges are given in Tables 1 and 2 for the frequency ranges 0.2–1 Hz, 1–3 Hz and 3–10 Hz. These frequency ranges are considered based on the fact

that the natural frequencies of multistorey buildings (3–10 floors) range between 1 and 3 Hz, whereas the natural frequencies for 1–3 storey buildings vary from 3 to 10 Hz. The frequency range 0.1–1 Hz is the natural frequency of more than 10 storey buildings (10–50 floors).

Site amplification has been computed using earthquake records at nine sites in the study area (Table 2 and Figure 6). Site amplification by microtremor records was computed at 30 sites. Results from nine sites are shown in Table 1 and Figure 5 for comparison with amplification computed by earthquake records at the respective sites. Results for the remaining sites are not given, as they show similar kind of amplification.

Site amplification in the frequency range 0.2–1 Hz, 1–3 Hz and 3–10 Hz using earthquake (microtremor) records for the study region are as follows: 0.8–4 (0.8–2), 0.8–4.4 (0.8–1.5) and 0.5–2 (1–1.7) respectively. Site amplification by microtremor records (Figure 5) show lesser amplification than that obtained from the earthquake records (Figure 6). Two peaks were observed in the site amplification obtained from the earthquake records, one at about 0.6 Hz and another at about 1.5 Hz. The peak at about 0.6 Hz was also observed in *H*/*V* obtained from the microtremor records. Generally, site amplifications estimated using microtremors are less reliable than those obtained from earthquake records. Microtremors provide a rough approximation of an earthquake site amplification[23].

Table 2. Site amplification using microtremor records

Site location	Amplification in frequency range		
	0.1–1 Hz	1–3 Hz	3–10 Hz
Site-4	0.8–2.2	0.6–2.0	0.7–1.3
Site-8	0.5–2.3	0.7–1.0	0.6–2.4
Site-17	0.4–3.5	0.5–1.0	0.9–1.1
Sitet-18	0.7–2.6	0.9–1.4	1.1–1.5
Site-24	0.9–2.3	0.7–1.1	0.6–2.1
Site-30	0.5–2.6	0.7–2.6	0.9–2.3
Site-31	0.5–3.3	0.6–1.2	0.8–1.3
Site-32	0.4–2.4	0.8–1.5	0.7–2.0
Site-33	0.4–2.4	0.7–1.3	0.7–1.7

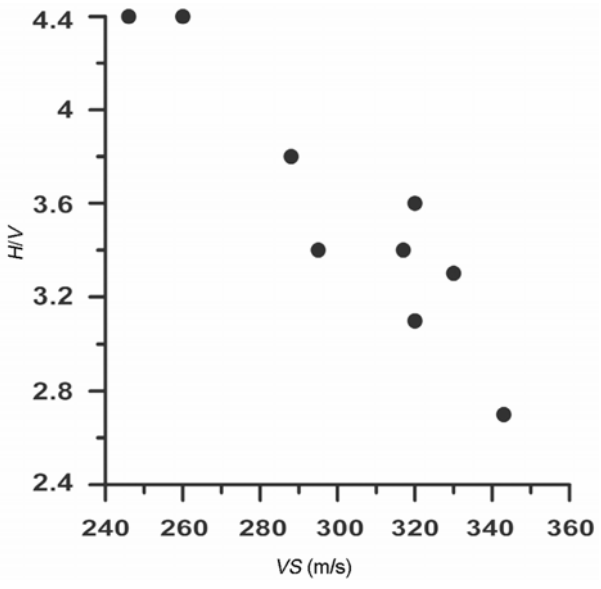

Figure 7. Site amplification versus *Vs*30.

The peak amplifications are related to sharp impedance contrast between layers and reveal the fundamental frequencies of layers below the recording site. The depth of the impedance contrast (*H*) is related to the short-wave velocity (*Vs*) and frequency of amplification *f* by $H = Vs/(4f)$. According to this equation, the peak amplification at 0.6 and 1.5 Hz is related to impedance contrast at greater and shallower depths respectively.

We have plotted maximum site amplification versus *Vs*30 in Figure 7. The plot shows good correlation, with site amplification increasing with decreasing *Vs*30. Sitewise *Vs*30 and site amplification at three different frequency ranges, viz. 0.1–1, 1–3 and 3–10 Hz are listed in Table 1. Site-17 and site-31 show higher site amplification (4.4 times) as these sites have the lowest *Vs*30 (about 250 m/s). The lowest amplification of 2.7 is found at site-32, which has the highest *Vs*30 (343 m/s) among sites of the study area. The remaining six sites show amplification in the range 3.4–3.8 times, where *Vs*30 is found in the range 288–330 m/s. From these observations, it is inferred that *Vs*30 is a proxy for site amplification.

Amplification up to 4.4 was observed in the frequency range 0.4–2.0 Hz which falls in the natural frequency range of multistorey buildings (more than three floors). This may lead to severe damage for such buildings in the study region if a strong regional earthquake or local earthquake of magnitude 6 occur. It is inferred from *Vs* measurements and site amplification that multistorey buildings of more than three floors in this region require careful designing.

1. Rastogi, B. K. *et al.*, The deadliest stable continental region earthquake occurred near Bhuj on 26 January 2001. *J. Seismol.*, 2001, **5**, 609–615.
2. Hough, S. E., Martin, S., Balham, R. and Atkinson, G. M., The 26 January 2001, *M* 7.6 Bhuj, India earthquake: observed and predicted ground motions. *Bull. Seismol. Soc. Am.*, 2002, **92**, 2061–2079.
3. Hunter, J. A., Benjumea, B., Harris, J. B., Miller, R. D., Pullan, S. E., Burns, R. and Good, R. L., Surface and down hole shear wave seismic methods for thick soil site investigations. *Soil Dyn. Earthq. Eng.*, 2002, **22**(9–12), 931–941.
4. NEHRP, NEHRP recommended provisions for seismic regulations for new buildings and other structures, Part 1: Provisions, Building Seismic Safety Council, Washington, DC, USA, 1997.
5. Uniform Building Code, International Conference of Building Officials, Whittier, CA, USA, 1997, p. 492.
6. Park, C. B., Miller, R. D. and Xia, J., Multichannel analysis of surface waves. *Geophysics*, 1999, **64**, 800–808.

7. Xia, J., Miller, R. D. and Park, C. B., Estimation of near-surface shear-wave velocity by inversion of Rayleigh waves. *Geophysics*, 1999, **64**, 691–700.
8. Richart, F. E., Hall, J. R. and Woods, R. D., *Vibrations of Soils and Foundations*, Prentice-Hall, 1970.
9. Xia, J., Miller, R. D. and Park, C. B., Advantages of calculating shear wave velocity from surface waves with higher modes, SEG, Expanded Abstracts, 2000.
10. Park, C. B., Miller, R. D. and Xia, J., Offset and resolution of dispersion curve in multichannel analysis of surface waves (MASW). In Proceedings of the SAGEEP, Denver, Colorado, RBA-6, 2001.
11. Ryden, N., Park, C., Miller, R., Xia, J. and Ivanov, J., High frequency MASW for non-destructive testing of pavements. In Proceedings of the Symposium on the Application of Geophysics to Engineering and Environmental Problems, Denver, Colorado, 4–7 March 2001.
12. Ivanov, J., Park, C. B., Miller, R. D. and Xia, J., Mapping Poission's ratio of unconsolidated materials from a joint analysis of surface-waves and refraction events. In Proceedings of the Symposium on the Application of Geophysics of Engineering and Environment Problems, Arlington, VA, 20–24 February 2000.
13. Park, C. B., Miller, R. D., Xia, J. and Ivanov, J., Multichannel analysis of underwater surface wave near B. C. Vancouver, Canada. In Proceedings of the 70th Annual International Meeting, SEG, Expanded Abstracts, 2000, pp. 1303–1306.
14. Miller, R. D., Xia, J., Park, C. B. and Ivanov, J., Multichannel analysis of surface waves to map bedrock. *Leading Edge*, 1999, **18**, 1392–1396.
15. Miller, R., Xia, J., Park, C. B., Davis, J., Shefchik, W. and Moore, L., Seismic techniques to delineate dissolution features in the upper 1000 ft at a power plant. In 69th Annual International Meeting, SEG, Expanded Abstracts, 1999, pp. 492–495.
16. FEMA, Multi hazard identification and assessment, Federal Emergency Management Agency, Washington DC, USA, 1997.
17. International Building Code, International Code Council, Falls Church, VA, 2000, 5th edn.
18. Konno, K. and Ohmachi, T., Ground motion characteristics estimated from spectral ratio between horizontal and vertical components of microtremor. *Bull. Seismol. Soc. Am.*, 1998, **88**(1), 228–241.
19. Bonilla, L. F., Steidl, J. H., Lindley, G. T., Tumarkin, A. G. and Archuleta, R. J., Site amplification in the San Fernando Valley, California; variability of site effect estimation using the *S*-wave, Coda, and *H*/*V* methods. *Bull. Seismol. Soc. Am.*, 1997, **87**(3), 710–730.
20. Field, E. and Jacob, E. H., A comparison and test of various site response techniques, including three that are non-reference-site dependent. *Bull. Seismol. Soc. Am.*, 1995, **85**, 1127–1143.
21. Castr, R. R., Mucciarelli, M., Pacor, F. and Petrungaro, C., *S*-wave site response using horizontal-to-vertical spectral ratios. *Bull. Seismol. Soc. Am.*, 1997, **87**(1), 256–260.
22. Bonilla, L. F., Steidl, J. H., Lindley, G. T., Tumarkin, A. G. and Archuleta, R. J., Borehole response studies at the Garner valley, southern California. *Bull. Seismol. Soc. Am.*, 2002, **92**(8), 3165–3379.
23. Lermo, J. and Chavez-Garcia, F. J., Are microtremors useful in site response evaluation? *Bull. Seismol. Soc. Am.*, 1994, **84**, 1350–1364.

ACKNOWLEDGEMENT. We thank Dr T. Sheshunarayan, NGRI, Hyderabad for guidance in the acquisition of data, processing and interpretation.

Received 9 December 2009; revised accepted 9 December 2010

Characterization of reflectance spectra of lunar analog rocks: gabbro and norite

S. Arivazhagan and S. Anbazhagan*

Department of Geology, Periyar University, Salem 636 011, India

Gabbro and noritic rocks are of particular interest to lunar scientists because they stratigraphically represent the deeper zones of the lunar crust. This communication reports reflectance spectra under 350–2500 nm for lunar analog rocks like gabbro and norite and a comparison with mineralogy and chemical composition. The gabbro and norite distinctly vary in terms of albedos of reflectance spectra. However, these rocks have common absorption bands in the visible–near infrared and SWIR spectral range. Norite has pyroxene absorption at 1072 nm, whereas this absorption is absent in gabbro. Similarly, the broader absorption band at 1200 nm in gabbro is probably due to overlapping absorption by crystalline plagioclase feldspar and the presence of pyroxene. Overall, minor variation in absorption bands, percentage of albedos and band depth are the diagnostic features useful for remote mapping of similar rock types on the lunar surface.

Keywords: Gabbro, norite, reflectance spectra, lunar analog.

A WIDE variety of rock types exist throughout the nearside crust of the moon. Major rock types identified from the reflectance spectra include noritic, anorthositic, gabbroic and troctolitic composition[1]. The lunar crust exhibits noritic composition with different amounts of pyroxene and/or brecciation alteration. Materials representing stratigraphically deeper zones (5–15 km) of the lunar crust are dominated by gabbros, anorthosites and troctolites, with less than a quarter of the areas exhibiting noritic composition[1]. The noritic character of lunar breccias and glasses was recognized during the study of Apollo 11 and 12 samples[2,3]. It is assumed that the lunar crust is stratified into distinct upper anorthositic and lower noritic layers[4]. The dominant rock type noticed across the interior of the South Pole-Aitken basin is of noritic composition[5], representing lower crust mafic suite. The lunar highland region comprises of >90% plagioclase (anorthite). In some cases between 10% and 22.5% mafic composition (orthopyroxene, clinopyroxene or olivine) with the remainder plagioclase (noritic anorthosite, gabbroic anorthosite and troctolitic anorthosite); or between 22.5% and 40% mafic with the remainder plagioclase (anorthositic norite, anorthositic gabbro and anorthositic troctolite), and more than 40% mafic (norite,

*For correspondence. (e-mail: anbu02@gmail.com)